PROCEEDINGS OF THE ROYAL SOCIETY B

rspb.royalsocietypublishing.org

Research

Cite this article: Bednaršek N, Feely RA, Reum JCP, Peterson B, Menkel J, Alin SR, Hales B. 2014 *Limacina helicina* shell dissolution as an indicator of declining habitat suitability owing to ocean acidification in the California Current Ecosystem. *Proc. R. Soc. B* **281**: 20140123.
http://dx.doi.org/10.1098/rspb.2014.0123

Received: 17 January 2014
Accepted: 2 April 2014

Subject Areas:
environmental science, ecology

Keywords:
pteropods, ocean acidification, dissolution, aragonite undersaturation, habitat reduction

Author for correspondence:
N. Bednaršek
e-mail: nina.bednarsek@noaa.gov

Electronic supplementary material is available at http://dx.doi.org/10.1098/rspb.2014.0123 or via http://rspb.royalsocietypublishing.org.

Royal Society Publishing

Limacina helicina shell dissolution as an indicator of declining habitat suitability owing to ocean acidification in the California Current Ecosystem

N. Bednaršek[1], R. A. Feely[1], J. C. P. Reum[2], B. Peterson[3], J. Menkel[4], S. R. Alin[1] and B. Hales[5]

[1]National Oceanic and Atmospheric Administration (NOAA), Pacific Marine Environmental Laboratory (PMEL), 7600 Sand Point Way NE, Seattle, WA 98115, USA
[2]Conservation Biology Division, Northwest Fisheries Science Center, National Marine Fisheries Service, National Oceanic and Atmospheric Administration (NOAA), 2725 Montlake Boulevard East, Seattle, WA 98112, USA
[3]NOAA NMFS NW Fisheries Science Center, 2030 SE Marine Science Drive, Newport, OR 97365, USA
[4]Oregon State University, Cooperative Institute for Marine Resources Studies, Hatfield Marine Science Center, 2030 SE Marine Science Drive, Newport, OR 97365, USA
[5]College of Earth, Ocean, and Atmospheric Sciences, Oregon State University, Corvallis, OR 97331, USA

Few studies to date have demonstrated widespread biological impacts of ocean acidification (OA) under conditions currently found in the natural environment. From a combined survey of physical and chemical water properties and biological sampling along the Washington–Oregon–California coast in August 2011, we show that large portions of the shelf waters are corrosive to pteropods in the natural environment. We show a strong positive correlation between the proportion of pteropod individuals with severe shell dissolution damage and the percentage of undersaturated water in the top 100 m with respect to aragonite. We found 53% of onshore individuals and 24% of offshore individuals on average to have severe dissolution damage. Relative to pre-industrial CO_2 concentrations, the extent of undersaturated waters in the top 100 m of the water column has increased over sixfold along the California Current Ecosystem (CCE). We estimate that the incidence of severe pteropod shell dissolution owing to anthropogenic OA has doubled in near shore habitats since pre-industrial conditions across this region and is on track to triple by 2050. These results demonstrate that habitat suitability for pteropods in the coastal CCE is declining. The observed impacts represent a baseline for future observations towards understanding broader scale OA effects.

1. Introduction

The release of carbon dioxide (CO_2) into the atmosphere from fossil fuel burning, cement production and deforestation processes has resulted in atmospheric CO_2 concentrations that have increased about 40% since the beginning of the industrial era [1,2]. The oceans have taken up approximately 28% of the total amount of CO_2 produced by human activities over this time-frame [1–3], causing a variety of chemical changes known as ocean acidification (OA). The process of OA has reduced the average surface ocean pH by about 0.1 and is expected to reduce average pH by another 0.3 units by the end of this century [4,5]. The rapid change in ocean chemistry is faster than at any time over the past 50 Myr [6]. This CO_2 uptake will lead to a reduction in the saturation state of seawater with respect to calcite and aragonite, which are the two most common polymorphs of calcium carbonate ($CaCO_3$) formed by marine organisms [5,7].

High-latitude areas of the open ocean will be the most affected by OA owing to the high solubility of CO_2 in cold waters [8–10]; however, the California Current Ecosystem (CCE) is already experiencing CO_2 concentrations similar to the projections for high-latitude regions, pointing towards enhanced vulnerability to OA [11–14]. This is, in part, owing to the natural process of upwelling, which

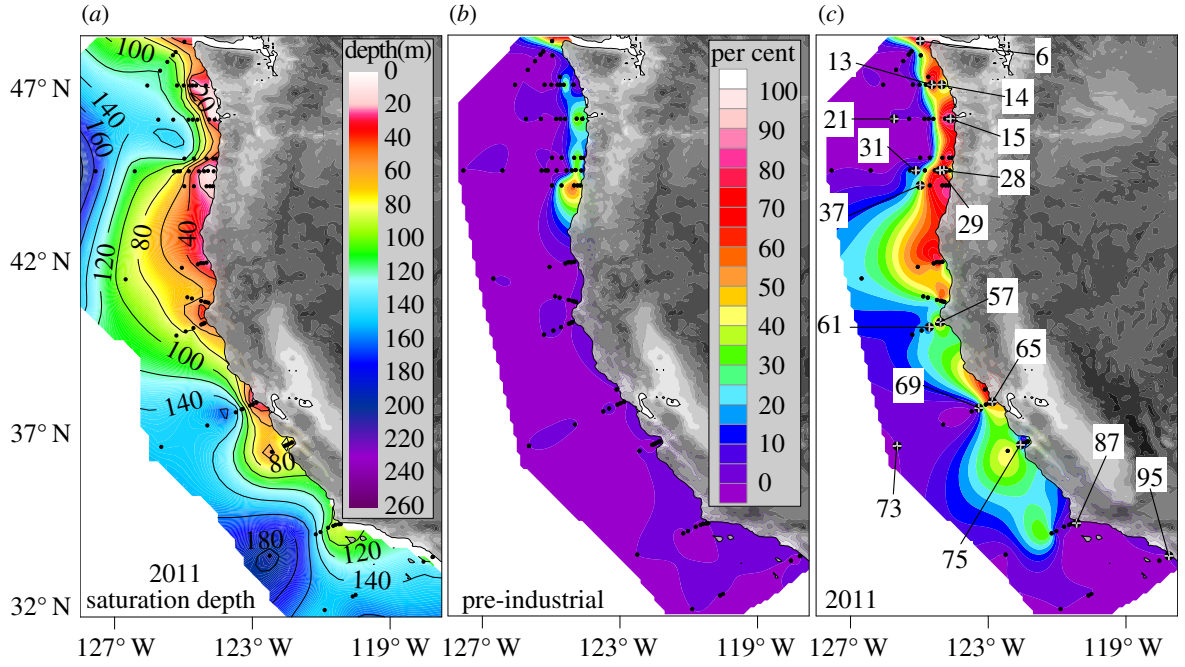

Figure 1. Planview maps. (*a*) Depth of the aragonite saturation horizon along the US West Coast. (*b*) Per cent of upper 100 m of the water column in the CCE estimated to be undersaturated during the (*b*) pre-industrial time and (*c*) the August–September 2011 time period. Pteropod station locations are indicated by numbers within the squares (*c*) and are referred to in figure 3.

brings already CO_2-rich waters from the ocean interior to the shelf environment and adds to the anthropogenic CO_2 contribution. These combined processes result in the greater frequency of thermodynamically unfavourable conditions [14,15], enhancing dissolution of $CaCO_3$ in the water column [16]. The term that quantifies the thermodynamic tendency towards dissolution or precipitation is the saturation state, or Ω_{ar} (omega); for a given $CaCO_3$ mineral, e.g. aragonite, $\Omega_{ar} = [Ca^{2+}][CO_3^{2-}]/K'_{spar}$, where $[Ca^{2+}]$ and $[CO_3^{2-}]$ are concentrations of calcium and carbonate ion, respectively, and K'_{spar} is the apparent solubility product for aragonite. When omega is greater than 1, precipitation is thermodynamically favoured, and when omega is less than 1, there is a thermodynamic tendency towards dissolution. Because of the combined effects of pressure and organic matter remineralization at depth, Ω_{ar} is typically lower at greater depths. The depth at which $\Omega_{ar} = 1$, known as the aragonite saturate horizon, has shoaled by as much as 25–40 m in upwelling shelf waters and approximately 40–100 m in offshore regions of the CCE [11,14]. The CCE is characterized by strong spatial (both horizontal and vertical) and temporal gradients in Ω_{ar} [11,14], with the aragonite saturation shoaling closest to the surface during the summer upwelling season in the Washington–Oregon coastal regions and off northern California. Based on both discrete observations and model calculations, it has been suggested that the upwelled undersaturated source-waters were present 10% of the time at the shelf break in the pre-industrial era, and contemporary ocean source-waters are undersaturated approximately 30% of the time during the upwelling season at the shelf break [12–14]. The upwelled undersaturated waters reach their shallowest depths close to the coast where they occasionally reach the surface [4,11,14]. The results for the 2011 cruise (figure 1*a*,*c*), which are representative of summertime conditions for the last few years, show evidence for corrosive water shoaling along the bottom to depths of about 20–50 m in the coastal waters off Washington, Oregon and northern California, and to depths of 60–120 m off southern California. The Washington–Oregon results are consistent with time-series measurements off Newport, Oregon, which provide evidence for increased fluctuations in Ω_{ar} (range: 0.8–3.8) on time-scales of weeks and very low saturation state waters during the upwelling season from June through to October [14,16]. From the moored saturation state and temperature observations from 2007 through to 2011, it is evident that the upwelling events primarily occur in the summer and early autumn months and last for approximately one to five weeks [14,16]. During this period, offshore surface waters generally have higher aragonite saturation states than the onshore waters (figure 1*a*,*c*). After the upwelling season has ended in November, the surface Ω_{ar} values average about 2.0 (range: 1.8–2.3) and show little variability during the winter and early spring months [14]. The anthropogenic component of the increased dissolved inorganic carbon (DIC) in the upwelled water contributes approximately 10–20% of the total change in Ω_{ar} during the upwelling season [14,16].

For the southern California region, the 2011 Ω_{ar} data in figure 1*a*,*c* are also consistent with the proxy-based 2005–2011 time series of Ω_{ar} data of Alin *et al.* [17] for the CalCOFI region off southern California, which suggest that the aragonite saturation horizon generally varies between depths of about 50–200 m and shows more spatial variability during the summer upwelling season. This makes the CCE an ideal ecosystem to study seasonally persistent OA conditions for better informed predictions of future impacts, especially for species that might be most vulnerable to more intensified and prolonged exposure to OA [18–20].

Pteropods are ubiquitous holoplanktonic calcifiers that are particularly important for their role in carbon flux and energy transfer in pelagic ecosystems. From an evolutionary perspective, a progressively thinner and lighter shell might have

provided pteropods with a competitive advantage for conquering new niches within the pelagic realm [21]. They build shells of aragonite, a more soluble form of $CaCO_3$, and contribute 20–42% towards global carbonate production [22], with higher biomasses in polar areas [23,24] as well as on the continental shelves and areas of high productivity [22]. The CCE includes shelf waters that are among the most biologically productive in the world [25], where the most ubiquitous pteropod species, *Limacina helicina*, can attain high abundances [26] and represent an important prey group for ecologically and economically important fishes, bird and whale diets [27]. Their spatial habitat stretches along the CCE and their vertical habitat encompasses the upper 75–150 m during day and night, with some healthy individuals capable of vertically migrating much deeper [28,29].

The CCE is a major upwelling region that is already experiencing 'acidified' conditions [11–14] under which thin pteropod shells are vulnerable to dissolution [30–32], even by short-term exposures (4–14 days) to near-saturated waters ($\Omega_{ar} \sim 1$), which makes them a suitable indicator for monitoring small-scale changes in the carbonate chemistry environment [30]. The existence of strong vertical gradients in aragonite saturation in the first 100 m of the CCE further accelerated by anthropogenic OA, where undersaturation protrudes into the pteropod vertical habitat provided a setting for estimating quantitative relationships between *in situ* undersaturation and shell dissolution. These quantitative relationships can further be used to evaluate potential changes in reduction of vertical habitat suitability for pteropods over time owing to OA.

2. Material and methods

(a) Carbonate chemistry sampling and analytical methods

For the 2011 West Coast OA (WCOA) cruise, samples were analysed for DIC, total alkalinity (TA) and hydrographic data along 13 cross-shelf transects (figure 1*a*), from 11 August to 3 September 2011. The conditions observed during the 2011 WCOA summer cruise were consistent with other observations and model results for the last several years during the upwelling season [11–17]. Water samples were collected from modified Niskin-type bottles and analysed for DIC, TA, oxygen, nutrients and dissolved and particulate organic carbon. The DIC concentration was determined by gas extraction and coulometry using a modified Single Operator Multi-parameter Metabolic Analyser, with a precision of ± 1.5 µmol kg^{-1}. Seawater TA was measured by acidimetric titration, employing the open-cell method described by Dickson *et al*. [33,34]. The precision for TA was ± 2.0 µmol kg^{-1}. Replicate samples were typically taken for two sample depths at each station. The replicate samples were interspersed throughout station depth for quality assurance. No systematic differences between the replicates were observed. Data accuracy was confirmed by regular analyses of certified reference materials [33].

Using the programme of Lewis & Wallace [35], carbonate ion concentration was calculated using carbonic acid dissociation constants of Lueker *et al*. [36]. The *in situ* degree of saturation of seawater with respect to aragonite and calcite is the ion product of the concentrations of calcium and carbonate ions, at the *in situ* temperature, salinity and pressure, divided by the apparent stoichiometric solubility product (K'_{spar}) for those conditions, where Ca^{2+} concentrations are estimated from the salinity, and carbonate ion concentrations are calculated from the DIC and TA data. The temperature and salinity effect on the solubility is estimated from the equation of Mucci [37] and includes the adjustments to the constants recommended by Millero [38].

(b) Physical–chemical background calculations

We used carbonate chemistry measurements obtained from discrete water samples to develop a linear model for estimating aragonite saturation state (Ω_{ar}) values across depths at each sampling station, based on conductivity, temperature and depth (CTD) depth profiles of oxygen concentrations and temperature. Although predictive algorithms of Ω_{ar} have been developed for the CCE using these variables [17,39], they are not valid for near-surface waters (less than 15 m) and were therefore not applied to our dataset. In preliminary models of Ω_{ar}, we evaluated multiple regression models where temperature and oxygen were included as predictor variables, but we observed residual error structure at the station level. To accommodate this issue and achieve better predictive performance, we fitted a mixed effects model for both variables (temperature (°C) and oxygen (µmol kg^{-1})). We used ln-transformed Ω_{ar} and O_2 to improve normality in the residual error. We evaluated model fit based on the proportion of variance explained by both the fixed and random effects (i.e. the 'conditional r^{2}') [40] and the root mean square error (RMSE). The final model had a conditional r^2 of 0.99 and a RMSE (based on the original Ω_{ar} scale) of 0.0016, indicating a strong fit to the data, and was subsequently used to predict Ω_{ar} across all depths (0–100 m) with corresponding CTD temperature and oxygen concentration measurements. The model was fitted using the 'nlme' statistical library and implemented in the 'R' statistical software package [41].

(c) Biological sampling

Sampling stations were located from 31 to 48° N and from 122 to 126° W (figure 1*a*,*c*). The survey encompassed three broad regions typified by regional differences in wind and temperature patterns that potentially affect the dynamics of Ω_{ar} [42]. The region north of Cape Mendocino (40.5° N) was denoted as the northern region, between Cape Mendocino and Point Conception (34.5° N) as the central region, and southward from Point Conception (32.4° N) as the southern region (figure 1*c*). Because each transect was conducted in a perpendicular orientation to the coastline, the stations farthest offshore along some transects may cross these boundaries. Onshore and offshore regions were delineated by the 200 m shelf break isobath. Pteropods were sampled using a 1 m diameter Bongo net with a 333 µm mesh net usually towed at a speed of two to three knots for approximately 30 min. As the upper 100 m of the water column is pteropod vertical migration habitat [29], sampling strategy was aimed at vertically integrating the first 100 m of water column. While different pteropod species were caught, only individuals of *L. helicina* were preserved and were subsequently counted and analysed for evidence of dissolution. To estimate abundance in the upper 100 m, the subsample (N) was taken from the original sample reporting counts as depth-integrated abundance (ind m^{-2}) (electronic supplementary material, table S1). For the purpose of the dissolution study, only live individuals were preserved in buffered formalin with pH ~ 8.4, which protected shells from further dissolution; 10 individuals on average were randomly picked from each preserved sample where *L. helicina* individuals were found, usually in the form of juveniles and subadults ranging in lengths from 0.5 to 2.5 mm. The analysed samples contained only forma *Limacina helicina helicina* f. *pacifica*, while f. *acuta* was excluded from analyses in order to not mix potentially genetically different populations. Upon visual inspection with a light microscope, we discarded the shells that were mechanically broken. In the process of shell preparation (described below), some of the shells are usually mechanically destroyed or damaged. Those were discarded and only intact shells were deemed suitable for scanning electron microscopy (SEM) shell analyses.

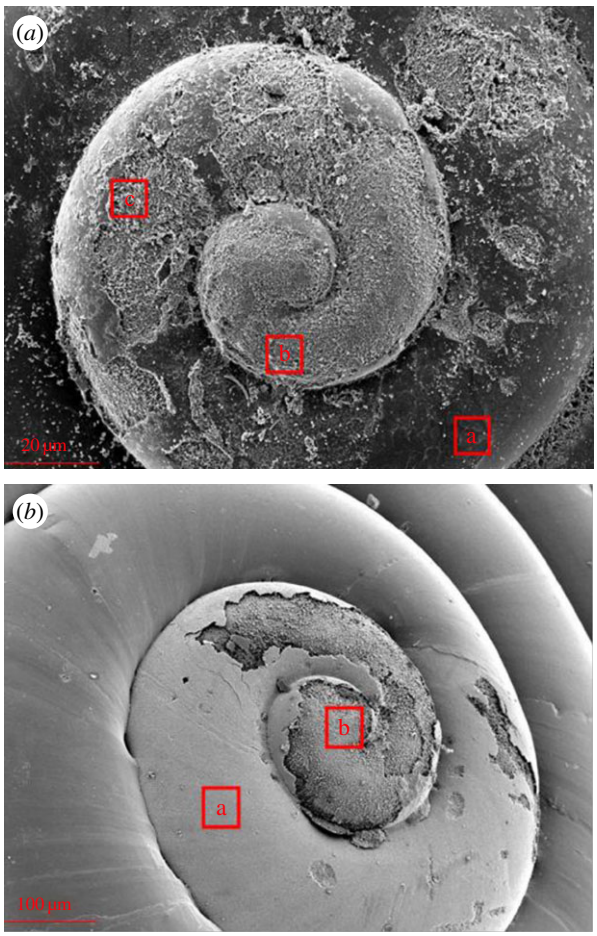

Figure 2. SEM images of shells of the pteropod *Limacina helicina helicina* f. *pacifica* sampled during the 2011 cruise showing signs of *in situ* dissolution from (*a*) an onshore station, with the entire shell affected by dissolution, and (*b*) from the offshore region, with only the protoconch (first whorl) affected. Indicated in the figure are: a, intact surface; b, Type I dissolution; and c, severe dissolution (Type II or Type III): see Material and methods for description of dissolution types. (Online version in colour.)

(d) Shell preparation

We used a non-invasive preparation method on preserved specimens to examine shell surfaces using SEM. A two-step preparation method of dehydration and drying is necessary in order to not introduce methodological artefacts of shell damage created by sheer forces under vacuum inside the SEM. Previous work demonstrated that the chemical treatments do not introduce any additional shell dissolution [30]. Second, plasma etching was applied to remove upper organic layers and expose the structural elements of the shell.

We categorized shell dissolution into three types based on the depth within the crystalline layer to which dissolution extended, following Bednaršek *et al.* [30]. Dissolution characterized by Type II and Type III damage impacts shell fragility [30], and we therefore referred to this kind of damage as severe (figure 2*a*).

(e) Statistical analysis

We evaluated whether the fraction of undersaturated waters in the top 100 m of the water column (as inferred from our model-based estimation of Ω_{ar}) was associated with the incidence of severe shell damage (Type II or Type III damage) in this natural habitat of pteropods. At onshore stations where bottom depths were shallower than 100 m, we estimated the fraction of the total water column that was undersaturated. We modelled the probability of observing severe shell damage using logistic regression where the response variable (severe damage present/not present) was treated as binomial (coded as 1 and 0, respectively) and the predictor variable (per cent undersaturation of the water column) was related to the response variable using a logit link function [43]. We tested whether the model containing the per cent undersaturation term was a significant improvement over the null model (intercept only) using a likelihood ratio test (see equation (3.1) in Results and discussion).

(f) Sensitivity study

We conducted a sensitivity study to evaluate potential differences in Ω_{ar} between present-day conditions and those assuming DIC levels corresponding to pre-industrial and future (2050) atmospheric CO_2 levels. For pre-industrial and future estimates, we assumed that the source-water DIC responded to air–sea CO_2 equilibrium conditions at the time of its last contact with the atmosphere, following Harris *et al.* [14]. Using a modified version of the Feely *et al.* [11] method for calculating Ω_{ar}, Harris *et al.* [14] (see the electronic supplementary material) calculated anthropogenic contribution to DIC to be approximately 53 µmol kg^{-1} during the summer upwelling time. To calculate Ω_{ar} values corresponding to pre-industrial DIC levels, we simply subtracted 53 µmol kg^{-1} from our *in situ* measurements of DIC and recalculated the carbonate system. This carries the implicit assumption that source-water alkalinity has been time-invariant, and that the respiratory modification of TA and DIC have also been constant over time. We estimated a potential anthropogenic contribution of 1.19 µmol kg^{-1} yr^{-1} to DIC or 46.4 µmol kg^{-1} increases in source-water DIC for 2050 based on an assumed continuation of an increasing trend in North Pacific surface water DIC [44]. This value was added to the 2011 DIC observations, and the Ω_{ar} values were calculated from those values and the 2011 TA. For both pre-industrial and future estimates of Ω_{ar}, we fit linear mixed effects models to predict values across depths based on CTD temperature and oxygen concentrations. From the predicted Ω_{ar} values, we estimated the percentage of the top 100 m of the water column that was undersaturated for comparison to present-day estimates. The linear mixed effects models of pre-industrial and 2050 Ω_{ar} fitted the data well (conditional r^2: 0.99 for both models) and exhibited low residual error (RMSE: 0.0013 and 0.0021, respectively).

3. Results and discussion

We collected and analysed samples originating from the National Oceanographic and Atmospheric Administration (NOAA) 2011 WCOA cruise, from northern Washington State to southern California from 11 August to 3 September 2011 (figure 1*a*). There is a large degree of variability of aragonite saturation state across regions within the CCE (figure 1*c*). Co-varying trends in temperature, salinity, oxygen and carbonate chemistry determine the depth of the aragonite saturation horizon ($\Omega_{ar} = 1$), represented as the depth of the undersaturated water (figure 1*a*) and the percentage of water undersaturated with respect to aragonite in the upper 100 m (figure 1*c*). To estimate the aragonite saturation state across the full water column, we used the fitted model to predict Ω_{ar} at all depths based on CTD temperature, salinity and oxygen sensor measurements, from which we calculated the vertically integrated percentage of undersaturation in the first 100 m based on the depth at which the aragonite saturation horizon occurred.

The coastal waters of the North American West Coast experience larger variability in carbonate chemistry as a result of several interacting processes, including seasonal upwelling, uptake of anthropogenic CO_2 and local respiratory

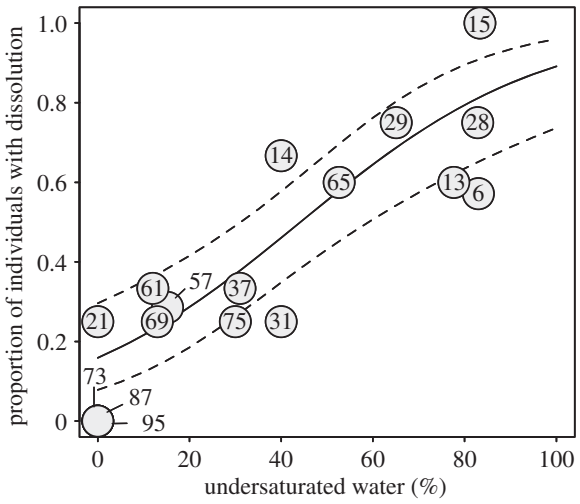

Figure 3. Proportion of pteropods with severe shell dissolution as a function of the percentage of the water column in the upper 100 m that is undersaturated with respect to aragonite. Station locations from figure 1*c* are shown with each symbol. The fitted regression line (solid line) and 95% prediction confidence band (dashed lines) are overlaid.

processes in water masses below the photic zone and nutrient overloads [45]. The seasonal upwelling along with bathymetric characteristics, such as wider shelves of the northern and central CCE, result in steep Ω_{ar} gradients across short depth intervals, though the gradients are much less pronounced over the narrow shelves in the southern CCE (figure 1*c*). Along the West Coast, low Ω_{ar} occurs in the late spring through to early autumn months, primarily from the seasonal upwelling of high CO_2 water from depths of about 80–200 m. By August, we observed, on average, 30% of the upper 100 m of the water column to be undersaturated, with a greater percentage of undersaturation occurring onshore relative to offshore stations (48% versus 13%, respectively; see Material and methods; figure 1*a*,*c* and table 1). The upwelled undersaturated waters reach their shallowest depths close to the coast [11,14] and undersaturated waters can exceed 50% of the upper 100 m of the water column (figure 1*c*). This general spatial pattern was evident throughout most of the CCE, except for onshore stations south of approximately 34° N that were generally supersaturated in the top 100 m and differed little from offshore stations (figure 1*c*; electronic supplementary material, figure S1). Electronic supplementary material, figure S1, shows the station-by-station profiles of Ω_{ar} with depth. In the northern and central onshore CCE stations (stations 6, 13, 14, 15, 28, 29, 57, 65, 87 and 95), the aragonite saturation horizon is located within the upper 20–50 m, while in the offshore stations (stations 21, 31 37, 57, 61 and 69), this occurs at about 80 m or deeper. Southern CCE offshore stations are similar to the northern and central offshore CCE stations in that the depth of undersaturation generally occurs below 80 m (stations 73 and 75), while in the southern onshore CCE stations, supersaturated conditions persist throughout the shallow water column (electronic supplementary material, figure S1), consistent with the Alin *et al.* [17] time-series results.

At the investigated stations, depth-integrated pteropod abundance and dissolution were determined. Pteropod populations show a considerable degree of regional variability in abundance, with depth-integrated abundances increasing from the southern part of the northern stations (see

Table 1. Mean percentage of the water column that was undersaturated with respect to aragonite and mean proportion of individuals with severe shell dissolution across all stations sampled during the 2011 West Coast survey under present-day conditions (2011) and assuming reductions (pre-industrial) and increases (2050) to *in situ* measurements of DIC. (The relationship estimated in figure 3 was used to estimate the probability of observing severe shell damage under *in situ* DIC concentrations measured in August 2011. Proportions were converted to percentages for clarity.)

	pre-industrial	2011	2050
percentage of undersaturated water (100 m)			
all stations	4	29	53
bottom depth < 200 m	8	48	72
bottom depth > 200 m	0	13	38
mean proportion of ind. with severe shell dissolution			
all stations	18	38	57
bottom depth < 200 m	21	53	71
bottom depth > 200 m	16	24	45

classifications of regions in Material and methods) to central onshore stations, where they can reach up to 14 000 ind m^{-2} (electronic supplementary material, table S1). Although the sampled stations were biased towards onshore stations, *L. helicina* was often present in high numbers in the offshore stations, as previously reported by Mackas & Galbraith [29].

In situ shell dissolution of *L. helicina* was the predominant feature observed in the live samples collected with a 333 µm mesh Bongo net at the peak of summer upwelling in August 2011. Shell dissolution was examined and demonstrated on preserved specimens using SEM after initial steps of dehydration and chemical drying. We observed shell dissolution at 14 out of 17 sites, i.e. 82% of all the investigated stations sampled along the CCE. The signatures of dissolution ranged from increased porosity and upper crystalline layer erosion (Type I) to severe types of dissolution affecting lower crystalline layers (Type II and Type III; see Material and methods). The latter dissolution types were considered severe as shell integrity was compromised and a fragile shell is more prone to damage (figure 2*a*).

Shell dissolution of *L. helicina* closely corresponded to carbonate chemistry conditions. We observed a strong positive relationship between the proportion of pteropods with severe dissolution and the percentage of undersaturated habitat in the top 100 m of the water column (log likelihood ratio test: $L = 23.1$, d.f. $= 1$, $p < 0.001$; figure 3). The fitted model (original response scale) took the form

$$y = \frac{e^{3.67(\pm 0.82)x - 1.66 \pm 0.40}}{1 + e^{3.67(\pm 0.82)x - 1.66 \pm 0.40}}, \quad (3.1)$$

where y is the proportion of individuals with severe shell dissolution, and x is the percentage of undersaturated waters in the top 100 m.

At stations where none of the top 100 m of the water column was undersaturated, almost no evidence of severe

dissolution was present (with the exception of station 21 where undersaturation started at 111 m). By contrast, higher percentages of water column undersaturation corresponded to an increase in the proportion of individuals with severe dissolution (figure 3), making this habitat less favourable for pteropods as it increases the tendency of their shell dissolution. Consequently, with further shoaling of the depth of undersaturation in the upper 100 m, pteropod vertical habitat suitability declines. Comparing the stations between offshore and onshore, we found 53% of onshore individuals and 24% of offshore individuals on average to have severe dissolution (table 1). *Limacina helicina* from onshore regions showed dissolution that was evenly spread over the entire surface of shells (figure 2*a*), while in offshore regions only the first whorl (protoconch) showed evidence of dissolution (figure 2*b*). This suggests that less corrosive offshore conditions only affected pteropods during early stages, while prolonged exposure to more severe undersaturated conditions in onshore regions resulted in dissolution covering the whole shell.

We used equation (3.1) to predict the proportion of individuals with severe shell dissolution under various proportions of undersaturated ($\Omega_{ar} < 1$) conditions, corresponding to the pre-industrial era and the years 2011 and 2050 across all stations in the survey, always referring to the conditions during the peak of the upwelling season in summer. For pre-industrial conditions, we assumed that the source-water DIC responded to air–sea CO_2 differences following Harris *et al.* [14], and subtracted 53 $\mu mol\ kg^{-1}$ from our year 2011 *in situ* DIC measurements. For the year 2050, the calculated 46 $\mu mol\ kg^{-1}$ increase in source-water DIC was based on an assumed continuation of an increasing trend in DIC in north Pacific surface water [44], which is consistent with the recent modelling results for this region [12,13].

Our estimates suggest a naturally occurring baseline of severe shell dissolution in approximately 20% of pteropod individuals in the CCE during the upwelling season under pre-industrial conditions. However, relative to pre-industrial CO_2 concentrations, the modern volume of undersaturated waters in the top 100 m of the water column has increased over sixfold along the CCE (figure 1*b*,*c* and table 1). Increased occurrence of undersaturated waters in 2011 is thus thought to correspond to higher severe shell dissolution relative to pre-industrial conditions, especially in the onshore regions of the CCE during the upwelling season. Onshore, 53% of pteropod individuals on average were affected by severe shell dissolution in August 2011; more than double the proportion calculated for the pre-industrial era (table 1). With the projected increase in anthropogenic CO_2 uptake by 2050 (see sensitivity study in Material and methods), we estimate that 72% of the top 100 m water column in onshore stations will be undersaturated. Our undersaturation-dissolution model suggests that progressive shoaling of the aragonite undersaturation horizon may result in 70% of individuals being affected by severe shell dissolution in 2050, or about a tripling of severe damage relative to the pre-industrial era throughout most of the coastal region (table 1).

Significant increases in vertical and spatial extent of conditions favouring pteropod shell dissolution are expected to make this habitat potentially unsuitable for pteropods. Although pteropods have been exposed to high CO_2 from seasonally persistent upwelling through evolution, we have not found any evidence of resilience to counteract the scale of dissolution observed currently. While dissolution in juvenile bivalves has been a significant factor for increased mortality [46], the link between undersaturation and dissolution-driven mortality in pteropods has not been directly confirmed. However, with the occurrence of high CO_2, increased dissolution combined with increased frailty [30–32,47] might compromise shell integrity to the extent where indirect effects of bacterial infection and acid–base balance would induce increased acute mortality [46]. The first bottleneck would primarily affect veligers and larvae, life stages where complete shell dissolution in the larvae can occur within two weeks upon exposure to undersaturation [48]. The lack of shell would lessen an individual's defence against predators, and the shell also plays an essential role in feeding, buoyancy control and pH regulation [49]. The shell is of particular importance later during the reproductive stage, when sperm are exchanged between individuals and need to be stored before fertilizing an egg [21], thus shell compromised by dissolution may hinder reproductive success.

Besides mechanistic explanations for dissolution-driven mortality, higher energy expenditure can come at a cost to the individual's energy budget, although this is also dependent on food availability and life stage [32,50]. Undersaturated conditions are known to elicit repair-calcification and changes in metabolic processes [51–53], with potentially long-term implications for growth, fecundity and fitness [54]. Evidence suggests that exceeding an individual's energy budget can change a pteropod's swimming behaviour, reduce their wing beat frequency and cause increased mortality owing to combined exposure to lower pH and salinity [55].

Therefore, the recent observed decline in *L. helicina* populations on the continental shelf of Vancouver Island [29], where we demonstrated high occurrence of severe shell dissolution, calls for more in-depth characterization of possible dissolution-related mortality [46]. Given the multitude of biological processes at important pteropod life stages that are potentially affected by increased shell dissolution, we suggest that dissolution provides an insight as a potential causal pathway for the observed pteropod decline. On the other hand, no population decline has been detected in the southern CCE [56], where our data indicate that extensive dissolution is lacking and reflect predominantly supersaturated conditions in comparison with the northern CCE, which is not specific only for this cruise survey period.

Biogeochemically, increased dissolution will reduce the ballasting effect of settling particles [57] and downward carbon fluxes [58] but increase TA in the upper water column [7]. By 2050, tripling in the costal regions of pteropod shell dissolution is expected to drive twice as much $CaCO_3$ dissolution, with potentially significant increases in TA within the upper water column. Use of pteropods as a sentinel species can prove to be indispensable for understanding future changes in the ocean carbon chemistry.

The decline of suitable habitat and demonstrable dissolution of biogenic carbonates as a response to the changes in the CCE is expected to have large and profound implications for the long-term biological and biogeochemical effects of CO_2 in the coastal waters of the Pacific northwest [12,13,20,59]. Dissolution impacts observed along the CCE are much more extensive spatially than previously reported for the Southern Ocean pteropods [31] and represent a baseline for future observations, where pteropod shell dissolution observations could have direct implications for understanding broader scale OA effects.

4. Conclusion

The highly productive CCE region provides an environment where *L. helicina* can occasionally reach high abundances [26], both offshore [29] and onshore. Prevalence of juveniles indicate coastal regions to also be their reproductive habitats (electronic supplementary material, table S1). This makes CCE a core habitat for sustainability of pteropod population, reflecting their importance in food webs as well as the regional biogeochemical carbonate cycle in the coastal waters of the CCE. However, these new results are among the first clearly indicating a direction towards declining habitat suitability for pteropods in the natural environment of the CCE owing to OA. This study demonstrates a strong positive relationship between the proportion of pteropods affected by severe dissolution and the percentage of undersaturated water in the upper 100 m of the water column. Our estimates suggest that the incidence of severe shell dissolution has already more than doubled relative to pre-industrial conditions and could increase to as much as 70% by 2050 along the northern and central onshore CCE. While pteropod populations might still thrive in offshore regions in the near future, continuous reduction of habitat availability in the onshore shelf regions will put pteropods at risk, with strong implications for their sustainability.

Acknowledgements. We would like to thank Jennifer Fisher and Cynthia Peacock for collecting samples during the cruise, as well as the officers and crew of the R/V *Wecoma*. Our thanks also go to Dana Greeley and Sandra Bigley for their help with the manuscript figures and editing.

Funding statement. This research was supported by the NOAA Ocean Acidification Program and the Pacific Marine Environmental Laboratory.

References

1. Sabine CL *et al*. 2004 The oceanic sink for anthropogenic CO_2. *Science* **305**, 367–371. (doi:10.1126/science.1097403)
2. Canadell JG *et al*. 2007 Contributions to accelerating atmospheric CO_2 growth from economic activity, carbon intensity, and efficiency of natural sinks. *Proc. Natl Acad. Sci. USA* **104**, 18 866–18 870. (doi:10.1073/pnas.0702737104)
3. Feely RA *et al*. 2013 Global ocean carbon cycle, in *State of the Climate in 2012*, Global Oceans. *Bull. Am. Meteorol. Soc.* **94**, S72–S75.
4. Feely RA, Doney SC, Cooley SR. 2009 Ocean acidification: present conditions and future changes in a high-CO_2 world. *Oceanography* **22**, 36–47. (doi:10.5670/oceanog.2009.95)
5. Doney SC, Fabry VJ, Feely RA, Kleypas JA. 2009 Ocean acidification: the other CO_2 problem. *Annu. Rev. Mar. Sci.* **1**, 169–192. (doi:10.1146/annurev.marine.010908.163834)
6. Hönisch B *et al*. 2012 The geological record of ocean acidification. *Science* **335**, 1058–1063. (doi:10.1126/science.1208277)
7. Feely RA *et al*. 2004 Impact of anthropogenic CO_2 on the $CaCO_3$ system in the oceans. *Science* **305**, 362–366. (doi:10.1126/science.1097329)
8. Orr JC *et al*. 2005 Anthropogenic ocean acidification over the twenty-first century and its impact on calcifying organisms. *Nature* **437**, 681–686. (doi:10.1038/nature04095)
9. Steinacher M, Joos F, Frolicher TL, Plattner G-K, Doney SC. 2009 Imminent ocean acidification in the Arctic projected with the NCAR global coupled carbon cycle-climate model. *Biogeosciences* **6**, 515–533. (doi:10.5194/bg-6-515-2009)
10. McNeil BI, Matear RJ. 2008 Southern ocean acidification: a tipping point at 450-ppm atmospheric CO_2. *Proc. Natl Acad. Sci. USA* **105**, 18 860–18 864. (doi:10.1073/pnas.0806318105)
11. Feely RA, Sabine CL, Hernández-Ayón JM, Ianson D, Hales B. 2008 Evidence for upwelling of corrosive 'acidified' water onto the continental shelf. *Science* **320**, 1490–1492. (doi:10.1126/science.1155676)
12. Hauri C *et al*. 2013 Spatiotemporal variability and long-term trends of ocean acidification in the California Current System. *Biogeosciences* **10**, 193–216. (doi:10.5194/bg-10-193-2013)
13. Gruber N *et al*. 2012 Rapid progression of ocean acidification in the California Current System. *Science* **337**, 220–223. (doi:10.1126/science.1216773)
14. Harris KE, DeGrandpre MD, Hales B. 2013 Aragonite saturation state dynamics in a coastal upwelling zone. *Geophys. Res. Lett.* **40**, 2720–2725. (doi:10.1002/grl.50460)
15. Juranek LW *et al*. 2009 A novel method for determination of aragonite saturation state on the continental shelf of central Oregon using multi-parameter relationships with hydrographic data. *Geophys. Res. Lett.* **36**, L24601. (doi:10.1029/2009GL040778)
16. Evans W, Hales B, Strutton PG. 2011 Seasonal cycle of surface ocean pCO_2 on the Oregon shelf. *J. Geophys. Res.* **116**, C05012. (doi:10.1029/2010JC006625)
17. Alin SR *et al*. 2012 Robust empirical relationships for estimating the carbonate system in the southern California Current System and application to CalCOFI hydrographic cruise data (2005–2011). *J. Geophys. Res.* **117**, C05033. (doi:10.1029/2011JC007511)
18. Fabry VJ, Seibel BA, Feely RA, Orr JC. 2008 Impacts of ocean acidification on marine fauna and ecosystem processes. *Ices J. Mar. Sci.* **65**, 414–432. (doi:10.1093/icesjms/fsn048)
19. Kroeker KJ *et al*. 2013 Impacts of ocean acidification on marine organisms: quantifying sensitivities and interaction with warming. *Global Change Biol.* **19**, 1884–1896. (doi:10.1111/gcb.12179)
20. Barton A, Hales B, Waldbusser GG, Langdon C, Feely RA. 2012 The Pacific oyster, *Crassostrea gigas*, shows negative correlation to naturally elevated carbon dioxide levels: Implications for near-term ocean acidification effects. *Limnol. Oceanogr.* **57**, 698–710. (doi:10.4319/lo.2012.57.3.0698)
21. Lalli CM, Gilmer RW. 1989 *Pelagic snails: the biology of holoplanktonic gastropod mollusks*. Stanford, CA: Stanford University Press.
22. Bednaršek N, Možina J, Vogt M, O'Brien C, Tarling GA. 2012 The global distribution of pteropods and their contribution to carbonate and carbon biomass in the modern ocean. *Earth Syst. Sci. Data* **4**, 167–186. (doi:10.5194/essd-4-167-2012)
23. Accornero A, Manno C, Esposito F, Gambi MC. 2003 The vertical flux of particulate matter in the polynya of Terra Nova Bay. Part II. Biological components. *Antarctic Sci.* **15**, 175–188. (doi:10.1017/S0954102003001214)
24. Bathmann UV, Noji TT, von Bodungen B. 1991 Sedimentation of pteropods in the Norwegian Sea in autumn. *Deep Sea Res. Part A* **38**, 1341–1360. (doi:10.1016/0198-0149(91)90031-A)
25. Muller-Karger FE *et al*. 2005 The importance of continental margins in the global carbon cycle. *Geophys. Res. Lett.* **32**, L01602. (doi:10.1029/2004GL021346)
26. McGowan JA. 1967 *Distributional atlas of pelagic molluscs in the California Current region*. CalCOFI Atlas no. 6. La Jolla, CA: Scripps Institution of Oceanography.
27. Armstrong JL *et al*. 2005 Distribution, size, and interannual, seasonal and diel food habits of northern Gulf of Alaska juvenile pink salmon, *Oncorhynchus gorbuscha*. *Deep Sea Res. Part II* **52**, 247–265. (doi:10.1016/j.dsr2.2004.09.019)
28. Mackas DL, Galbraith MD. 2001 Zooplankton distribution and dynamics in a North Pacific eddy of coastal origin. 1. Transport and loss of continental margin species. *Jpn J. Oceanogr.* **58**, 725–738. (doi:10.1023/A:1022802625242)
29. Mackas DL, Galbraith MD. 2012 Pteropod time-series from the NE Pacific. *Ices J. Mar. Sci.* **69**, 448–459. (doi:10.1093/icesjms/fsr163)

30. Bednaršek N *et al*. 2012 Description and quantification of pteropod shell dissolution: a sensitive bioindicator of ocean acidification. *Glob. Change Biol.* **18**, 2378–2388. (doi:10.1111/j.1365-2486.2012.02668.x)
31. Bednaršek N *et al*. 2012 Extensive dissolution of live pteropods in the Southern Ocean. *Nat. Geosci.* **5**, 881–885. (doi:10.1038/ngeo1635)
32. Lischka S, Riebesell U. 2012 Synergistic effects of ocean acidification and warming on overwintering pteropods in the Arctic. *Glob. Change Biol.* **18**, 3517–3528. (doi:10.1111/gcb.12020)
33. Dickson AG, Afgan JD, Anderson GC. 2003 Reference materials for oceanic CO_2 analysis: a method for the certification of total alkalinity. *Mar. Chem.* **80**, 185–197. (doi:10.1016/S0304-4203(02)00133-0)
34. Dickson AG, Sabine CL, Christian JR. (eds) 2007 Guide to best practices for ocean CO_2 measurements. PICES Special Publication 3, IOCCP Report No 8. Sidney, BC: North Pacific Marine Science Organization.
35. Lewis E, Wallace DWR. 1998 Program developed for CO_2 system calculations. Technical Report ORNL/CDIAC-105. Carbon Dioxide Information Analysis Center, Oak Ridge National Laboratory, US Department of Energy, Oak Ridge, TN, USA.
36. Lueker TJ, Dickson AG, Keeling CD. 2000 Ocean pCO_2 calculated from dissolved inorganic carbon. *Mar. Chem.* **70**, 105–119. (doi:10.1016/S0304-4203(00)00022-0)
37. Mucci A. 1983 The solubility of calcite and aragonite in seawater at various salinities, temperatures, and one atmosphere total pressure. *Am. J. Sci.* **283**, 781–799. (doi:10.2475/ajs.283.7.780)
38. Millero FJ. 1995 Thermodynamics of the carbon dioxide system in the oceans. *Geochim. Cosmochim. Acta* **59**, 661–677. (doi:10.1016/0016-7037(94)00354-O)
39. Willette TM *et al*. 2001 Ecological processes influencing mortality of juvenile pink salmon (*Oncorhynchus gorbuscha*) in Prince William Sound, Alaska. *Fish. Oceanogr.* **10**, 14–41. (doi:10.1046/j.1054-6006.2001.00043.x)
40. Nakagawa S, Schielzeth H. 2013 A general and simple method for obtaining R^2 from generalized linear mixed-effects models. *Methods Ecol. Evol.* **4**, 133–142. (doi:10.1111/j.2041-210x.2012.00261.x)
41. R Development Core Team. 2008 *R: a language and environment for statistical computing*. Vienna, Austria: R Foundation for Statistical Computing.
42. Dorman CE, Winant CD. 1995 Buoy observation of the atmosphere along the west coast of the United States, 1981–1990. *J. Geophys. Res.* **100**, 16 029–16 044. (doi:10.1029/95JC00964)
43. Kutner M, Nachtsheim C, Neter J, Li W. 2004 *Applied linear statistical models*. New York, NY: McGraw-Hill/Irwin.
44. Dore JE, Lukas R, Sadler DW, Karl DM. 2003 Climate-driven changes to the atmospheric CO_2 sink in the subtropical North Pacific Ocean. *Nature* **424**, 754–757. (doi:10.1038/nature01885)
45. Feely RA *et al*. 2012 Decadal changes in the aragonite and calcite saturation state of the Pacific Ocean. *Glob. Biogeochem. Cycles* **26**, GB3001. (doi:10.1029/2011GB004157)
46. Green MA, Waldbusser GG, Reilly SL, Emerson K, O'Donnell S. 2009 Death by dissolution: sediment saturation state as a mortality factor for juvenile bivalves. *Limnol. Oceanogr.* **54**, 1037–1047. (doi:10.4319/lo.2009.54.4.1037)
47. Comeau S, Gorsky G, Jeffree R, Teyssié JL, Gattuso J-P. 2009 Impact of ocean acidification on a key Arctic pelagic mollusc (*Limacina helicina*). *Biogeosciences* **6**, 1877–1882. (doi:10.5194/bg-6-1877-2009)
48. Comeau S, Gorsky G, Alliouane S, Gattuso J-P. 2010 Larvae of the pteropod *Cavolinia inflexa* exposed to aragonite undersaturation are viable but shell-less. *Mar. Biol.* **157**, 2341–2345. (doi:10.1007/s00227-010-1493-6)
49. Simkiss K, Wilbur KM. 1989 *Biomineralization: cell biology and mineral deposition*. San Diego, CA: Academic Press.
50. Thomsen J, Casties I, Pansch C, Körtzinger A, Meltzner F. 2013 Food availability outweighs ocean acidification effects in juvenile *Mytilus edulis*: laboratory and field experiments. *Glob. Change Biol.* **19**, 1017–1027. (doi:10.1111/gcb.12109)
51. Seibel BA, Maas AE, Dierssen HM. 2012 Energetic plasticity underlies a variable response to ocean acidification in the pteropod, *Limacina helicina antarctica*. *PLoS ONE* **7**, e30464. (doi:10.1371/journal.pone.0030464)
52. Comeau S, Jeffree R, Teyssie JL, Gattuso J-P. 2010 Response of the Arctic pteropod *Limacina helicina* to projected future environmental conditions. *PLoS ONE* **5**, e11362. (doi:10.1371/journal.pone.0011362)
53. Lischka S, Büdenbender J, Boxhammer T, Riebesell U. 2011 Impact of ocean acidification and elevated temperatures on early juveniles of the polar shelled pteropod *Limacina helicina*: mortality, shell degradation, and shell growth. *Biogeosciences* **8**, 919–932. (doi:10.5194/bg-8-919-2011)
54. Wood HL, Spicer JI, Widdicombe S. 2008 Ocean acidification may increase calcification rates, but at a cost. *Proc. R. Soc. B* **275**, 1767–1773. (doi:10.1098/rspb.2008.0343)
55. Manno C, Morata N, Primicerio R. 2012 *Limacina retroversa's* response to combined effects of ocean acidification and sea water freshening. *Estuar. Coast. Shelf Sci.* **113**, 163–171. (doi:10.1016/j.ecss.2012.07.019)
56. Ohman MD, Lavaniegos BE, Townsend AW. 2009 Multi-decadal variations in calcareous holozooplankton in the California Current System: thecosome pteropods, heteropods, and foraminifera. *Geophys. Res. Lett.* **36**, L18608. (doi:10.1029/2009GL039901)
57. Klaas C, Archer DE. 2002 Association of sinking organic matter with various types of mineral ballast in the deep sea: implications for the rain ratio. *Global Biogeochem. Cycles* **16**, 63-1–63-14. (doi:10.1029/2001GB001765)
58. Betzer PR *et al*. 1984 The oceanic carbonate system: a reassessment of biogenic controls. *Science* **226**, 1074–1077. (doi:10.1126/science.226.4678.1074)
59. Waldbusser GG *et al*. 2013 A developmental and energetic basis linking larval oyster shell formation to acidification sensitivity. *Geophys. Res. Lett.* **40**, 2171–2176. (doi:10.1002/grl.50449)